Progress In Electromagnetics Research, PIER 100, 245–263, 2010

APPLICATION OF THE IMPROVED MATRIX TYPE FDTD METHOD FOR ACTIVE ANTENNA ANALYSIS

S.-Q. Xiao, Z. H. Shao, and B.-Z. Wang

Institute of Applied Physics
University of Electronic Science and Technology of China
Chengdu 610054, China

Abstract—An improved finite-difference time-domain (FDTD) method has been extended to analyze the antennas with complicated lumped/active networks in this paper. The improved FDTD method is based on a novel integral transform and the matrix theory. Combining the novel integral transform with Kirchhoff's circuit laws, the hybrid networks comprised of high order linear and nonlinear elements with arbitrary connection can be modeled by a stable matrix equation. An effective model is built for linear lumped networks including internal independent sources. A wire antenna loaded with wideband match network and a two-element active patch antenna loaded with Gunn diodes are analyzed by the developed techniques. The analysis results indicate that the improved matrix-type FDTD method is not only stable and accurate, but also time-saving in simulating the complicated hybrid networks.

1. INTRODUCTION

There are several methods to analyze electromagnetic characteristics of microwave and antenna structures, such as method of moment (MOM), finite-difference time-domain (FDTD) method, finite element method (FEM), etc. [1–3]. The FDTD method is one of the good candidates to model the electromagnetic structures because it can provide an efficient and powerful global analysis [4–7]. Lump and active circuits play an important role in microwave and antenna systems. In modern RF front-end systems, lots of lumped and active devices, such as chip resistors, diodes and FETs, are integrated with passive circuits tightly. In antenna applications, active antenna concept has been used extensively, and lumped and active element loading has become a critical technique to improve the antenna characteristics, e.g.,

Corresponding author: S.-Q. Xiao (xiaoshaoqiu@uestc.edu.cn).

enhance antenna bandwidth and reduce antenna size [8], etc. When the FDTD method is used to analyze these microwave circuits and antenna systems, one of the most difficult challenges is to construct the models for these lumped and active circuit units.

A so-called lumped-element FDTD method has been presented to simulate single lumped elements such as resistors, inductors, capacitors, and also diodes and transistors with very simple equivalent models [9]. Its main limitation is that it cannot account for two-terminal circuit consisting of arbitrary connection of several lumped elements. To improve its application, a recent literature [10] has developed an approach to treat the arbitrary linear lumped network, where the networks are described in terms of its impedance in Laplace domain and then transformed to Z-domain by the bilinear transformation. The time domain port voltage of the linear lumped networks required by Yee's cell can be obtained by using appropriate digital signal processing techniques. More recently, Wu et al. [11] have proposed another method to incorporate arbitrary high order linear lumped networks into FDTD method. These methods in [10, 11] are based on explicit iterative techniques to treat linear lumped network. In order to create an explicit iterative formula, in literature [11] a complex recursion technology has been used. However, these methods in [10, 11] cannot be utilized to analyze linear lumped networks including internal independent sources and active elements. For overcoming the disadvantages in [9–11], a matrix method based on Kirchhoff's circuit laws developed in the literature [12] can be used to model linear lumped and active networks, whereas it is very difficult to use this method to deal with the networks in which some elements expressed by high order linear equations are included.

In this paper, the effective FDTD models are presented based on literature [13] to simulate complex hybrid networks which consist of independent sources, nonlinear elements and the elements expressed by high order linear equations. The effective models are applied to analyze the active antenna and show their potential value.

2. THE BASIC THEORY OF THE IMPROVED MATRIX METHOD

2.1. The Matrix Method for Linear Lumped Network

The frequency dependent impedance of a linear lumped network is described in integral form of the rational function as [11]

$$\frac{V_0(s)}{I_0(s)} = \frac{\sum_{r=0}^{R} a_r \left(1/s\right)^r}{\sum_{m=0}^{M} b_m \left(1/s\right)^m} \tag{1}$$

where, V_0 and I_0 are the terminal voltage and current, $s = j\omega$. R and M with the relationship of $|R - M| \leq 1$ are the order nominator and denominator of the rational function, respectively. The coefficients a_r and b_m are determined by lumped network.

Formula (1) can be rewritten as

$$\sum\nolimits_{m=0}^{M} b_m \, (1/s)^m V_0(s) = \sum\nolimits_{r=0}^{R} a_r \, (1/s)^r I_0(s) \tag{2}$$

Using Laplace-transform relationship between s-domain and time domain

$$F(s)/s \leftrightarrow \int_0^t f(\tau) d\tau, \tag{3}$$

and the improved finite integration (5) [13], Equation (2) can be discretized as follows

$$b_0 V_0^{n+1} + \sum\nolimits_{m=1}^{M} b_m (\Delta t)^m V_{0m}^{n+1} = a_0 I_0^{n+1/2} + \sum\nolimits_{r=1}^{R} a_r (\Delta t)^r I_{0r}^{n+1/2} \tag{4}$$

where, Δt is the time increment and

$$\begin{aligned}
V_{01}^{n+1} &= \frac{1}{\Delta t} \int_0^{(n+1)\Delta t} V_0(\tau) d\tau \\
&= \frac{1}{\Delta t} \int_0^{n\Delta t} V_0(\tau) d\tau + \frac{1}{\Delta t} \int_{n\Delta t}^{(n+1)\Delta t} V_0(\tau) d\tau \\
&= V_{01}^n + \frac{V_0^{n+1} + V_0^n}{2} && \text{(5a)} \\
V_{02}^{n+1} &= V_{02}^n + \frac{V_{01}^{n+1} + V_{01}^n}{2} && \text{(5b)} \\
&\cdots \\
V_{0M}^{n+1} &= V_{0M}^n + \frac{V_{0(M-1)}^{n+1} + V_{0(M-1)}^n}{2} && \text{(5c)} \\
I_{01}^{n+1/2} &= \frac{1}{\Delta t} \int_0^{(n+1/2)\Delta t} I_0(\tau) d\tau \\
&= I_{01}^{n-1/2} + \frac{I_0^{n+1/2} + I_0^{n-1/2}}{2} && \text{(5d)} \\
I_{02}^{n+1/2} &= I_{02}^{n-1/2} + \frac{I_{01}^{n+1/2} + I_{01}^{n-1/2}}{2} && \text{(5e)} \\
&\cdots \\
I_{0R}^{n+1/2} &= I_{0R}^{n-1/2} + \frac{I_{0(R-1)}^{n+1/2} + I_{0(R-1)}^{n-1/2}}{2} && \text{(5f)}
\end{aligned}$$

The finite integration (5) has been presented by Shao et al. to analyze the linear lump element-loaded microstrip hybrid circuit [13].

According to the traditional finite integration introduced in [11], Equation (2) is discretized as

$$b_0 V_0^{'n+1} + \sum\nolimits_{m=1}^{M} b_m V_{0m}^{'n+1} = a_0 I_0^{'n+1/2} + \sum\nolimits_{r=1}^{R} a_r I_{0r}^{'n+1/2} \tag{6}$$

where

$$\begin{aligned} V_{01}^{'n+1} &= \int_0^{(n+1)\Delta t} V_0(\tau) d\tau \\ &= \int_0^{n\Delta t} V_0(\tau) d\tau + \int_{n\Delta t}^{(n+1)\Delta t} V_0(\tau) d\tau \\ &= V_{01}^{'n} + \Delta t V_0^{'n+1} \end{aligned} \tag{7a}$$

$$\cdots$$

$$V_{0m}^{'n+1} = V_{0m}^{'n} + \Delta t V_{0(m-1)}^{'n+1} \quad (2 \le m \le M) \tag{7b}$$

$$I_{01}^{'n+1/2} = I_{01}^{'n-1/2} + \Delta t I_0^{'n+1/2} \tag{7c}$$

$$\cdots$$

$$I_{0r}^{'n+1/2} = I_{0r}^{'n-1/2} + \Delta t I_{0(r-1)}^{'n+1/2} \quad (2 \le r \le R) \tag{7d}$$

It can be seen that an additional factor of $1/\Delta t$ is multiplied at the right side of the novel integral transform (5) compared with the traditional one (7).

In linear, lossless and homogeneous medium, the coupling among the electric field $\mathbf{E}$, magnetic field $\mathbf{H}$ and current density $\mathbf{J}$ satisfies the following curl equation

$$\varepsilon \boldsymbol{\partial} \mathbf{E} / \partial t = \boldsymbol{\nabla} \times \mathbf{H} - \mathbf{J} \tag{8}$$

when lumped network occupies only one Yee's cell along x-direction, the coupling between the electromagnetic fields and the current I_0 passing through the lumped network can be written as

$$E_x^{n+1} = E_x^n + \Delta t / \varepsilon (\boldsymbol{\nabla} \times \mathbf{H})_x^{n+1/2} - \Delta t / \varepsilon \cdot I_0^{n+1/2} / (\Delta y \Delta z) \tag{9}$$

The relationship between local electronic field and port voltage of the lumped network is

$$V_0^{n+1} = E_x^{n+1} \Delta x \tag{10}$$

where Δx, Δy and Δz are the spatial increment along x-, y- and z-directions, respectively. From Equations (4), (5), (9), and (10), it is seen that an equations set can be constructed with $(M + R + 3)$ equations to solve $(M + R + 3)$ unknowns. The equations set can be written as a matrix format

$$\mathbf{AB} = \mathbf{C_0} \tag{11}$$

where, $\mathbf{A}$ is the $(M+R+3)\times(M+R+3)$ cofactor matrix,

$$\mathbf{A}=\begin{bmatrix}
1 & 0 & & & & & \Delta t/\varepsilon/(\Delta y\Delta z) & & 0 & \\
-\Delta x & 1 & & & & & & & & \\
0 & -\frac{1}{2} & 1 & 0 & & \cdots & 0 & & & \\
0 & 0 & -\frac{1}{2} & 1 & 0 & \cdots & 0 & & \cdots & \\
 & & & & & \cdots & & & & \\
0 & 0 & & \cdots & -\frac{1}{2} & 1 & 0 & & & \\
0 & b_0 & b_1\Delta t & \cdots & b_M(\Delta t)^M & & -a_0 & -a_1\Delta t & \cdots & -a_R(\Delta t)^R \\
0 & 0 & & \cdots & & & -\frac{1}{2} & 1 & \cdots & 0 \\
0 & 0 & & \cdots & & & & -\frac{1}{2} \quad 1 & \cdots & 0 \\
 & & \cdots & & & & & & & \\
0 & & \cdots & & & & & & -\frac{1}{2} & 1
\end{bmatrix} \tag{12}$$

$\mathbf{B}$ is the unknowns vector $(E_x^{n+1},\ V_0^{n+1},\ V_{01}^{n+1},\ \ldots,\ V_{0M}^{n+1},\ I_0^{n+1/2},\ I_{01}^{n+1/2},\ \ldots,\ I_{0R}^{n+1/2})^T$, and $\mathbf{C_0}$ is the constant vector

$$\begin{aligned}\mathrm{C}_0=\Bigg[&E_x^n+\frac{\Delta t}{\varepsilon}(\boldsymbol{\nabla}\times\mathbf{H})_x^{n+1/2} \quad 0 \quad \frac{V_0^n}{2}+V_{01}^n \\ &\cdots \frac{V_{0(M-1)}^n}{2}+V_{0M}^n \quad 0 \quad \frac{I_0^{n-1/2}}{2}+I_{01}^{n-1/2} \\ &\cdots \frac{I_{0(R-1)}^{n-1/2}}{2}+I_{0R}^{n-1/2}\Bigg]^T\end{aligned} \tag{13}$$

Based on the traditional finite integration (6) and (7), a similar equations set with (11) and a cofactor matrix $\mathbf{A}'$ can be obtained. Literature [13] has demonstrated the solution of the equations set of (11), which exists because of non-zero determinant of matrix $\mathbf{A}$, and matrix $\mathbf{A}$ is more well-conditioned than matrix $\mathbf{A}'$. Thereby, it is very easy to solve the electronic field on the Yee's cell occupied by linear lumped network. The examples in Section 3 will validate this nature numerically.

2.2. Matrix Method for Linear Lumped Network Including Internal Independent Sources

Based on the FDTD method introduced above, the analysis of linear lumped networks has been simplified. However, Formula (1) cannot be applied to calculate the impedance of linear lumped networks in which independent currents or voltage sources are included. According to the circuit equivalent principle, a linear lumped network including internal independent sources can be equivalent to Norton or Thevenin equivalent forms, as shown in Figs. 1(a) and (b), respectively. In Fig. 1,

I_{so} is Norton equivalent current source and V_{so} Thevenin equivalent voltage source. The passive lumped network can be obtained by shorting the internal voltage sources and opening the internal current sources in the original network.

Therefore, from the equivalent principle, the total current and terminal voltage of the linear lumped network in which k independent current/voltage sources are included can be connected with the expressions

$$Z_{nos} = \frac{V_0(s)}{I_0(s) + \sum_{k=1}^{K} I_{so}^k(s)} = \frac{\sum_{r=0}^{R} a_r \, (1/s)^r}{\sum_{m=0}^{M} b_m \, (1/s)^m} \tag{14a}$$

$$\text{or} \quad Z_{nos} = \frac{V_0(s) - \sum_{k=1}^{K} V_{so}^k(s)}{I_0(s)} = \frac{\sum_{r=0}^{R} a_r \, (1/s)^r}{\sum_{m=0}^{M} b_m \, (1/s)^m} \tag{14b}$$

where, Z_{nos} is the impedance of the passive lumped network; I_{so}^k and V_{so}^k are the Norton equivalent current source and Thevenin equivalent voltage source of the k-th internal independent sources, respectively.

Here, we only corporate Formula (14a) into the matrix type FDTD method to analyze linear lumped network with internal independent sources. Formula (14b) can be utilized by the similar procedure.

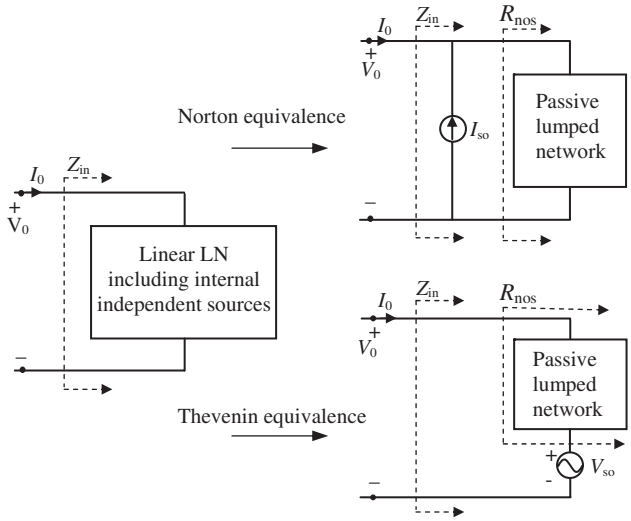

Figure 1. Equivalent models of the linear lumped network including internal independent sources.

Formula (14a) can be re-written as

$$V_0(s)\sum_{m=0}^{M} b_m\,(1/s)^m \;=\; I_0(s)\sum_{r=0}^{R} a_r\,(1/s)^r + \sum_{k=1}^{K}\cdot\sum_{r=0}^{R} a_r I_{so}^k(s)\,(1/s)^r \quad (15)$$

According to Equations (3)–(5), Equation (15) is transformed into time domain and then is discretized as

$$\begin{aligned} & b_0 V_0^{n+1} + \sum_{m=1}^{M} b_m(\Delta t)^m V_{0m}^{n+1} \\ & - \sum_{k=1}^{K}\cdot\sum_{r=0}^{R}\left\{F^{-1}\left[a_r I_{so}^k(s)\,(1/s)^r\right]\right\}^{n+1} \\ & = a_0 I_0^{n+1/2} + \sum_{r=1}^{R} a_r(\Delta t)^r I_{0r}^{n+1/2} \end{aligned} \quad (16)$$

$F^{-1}(\bullet)$ is the operator of the inverse Fourier transform. Using Equations (5), (9), (10), and (16), a new equations set as (11) can be established, where the known volume matrix $\mathbf{C}_0$ is changed as

$$\begin{aligned} \mathrm{C}_0^s = \Bigg[& E_x^n + \frac{\Delta t}{\varepsilon}(\boldsymbol{\nabla}\times\mathbf{H})_x^{n+1/2} \quad 0 \quad \frac{V_0^n}{2} + V_{01}^n \\ & \cdots \frac{V_{0(M-1)}^n}{2} + V_{0M}^n - \sum_{r=0,k=1}^{R,K}\left\{F^{-1}\left[a_r I_{so}^k\,(1/s)^r\right]\right\}^{n+1} \\ & \frac{I_0^{n-1/2}}{2} + I_{01}^{n-1/2} \quad \cdots \quad \frac{I_{0(R-1)}^{n-1/2}}{2} + I_{0R}^{n-1/2} \Bigg]^T \end{aligned} \quad (17)$$

In Equation (17), the $(M+3)$-th item, i.e., the source item, can be computed from the known internal independent sources and network structures. Thus, the electronic field on the Yee's cell occupied by linear lumped network with internal independent sources can be solved easily.

2.3. Matrix Method for Complex Linear Lumped Networks Based on Kirchhoff's Circuit Laws

The methods introduced in Subsections 2.1 and 2.2 require that impedance expression of linear lumped network be described by an equation about port current and voltage. In some cases, it is very troublesome even difficult to obtain a impedance expression for complicate linear lumped networks. An improved method can be used to avoid this difficulty. Based on Kirchhoff's current and voltage laws, a circuit equations set about the nodal voltage and branch current can be

extracted from the network topology. Combining it with Equations (4), (5), (9), and (10), a novel equations set as (11) can be established. In this procedure, each internal independent current/voltage sources is just connected with one equation.

Traditionally, when Kirchhoff's laws are used to analyze linear lumped network with the matrix method [12], the order of each element in the network and each equation in the equations set are required to be zero or one. However, using Kirchhoff's laws in conjunction with the new integral transform technique in (4) and (5), the network having the subcircuits expressed by high order equations can also be analyzed. The improved transform (4) and (5) should be used not only to discretize the time domain integration expresses, but also to describe the relationship between the current and voltage of each high order subcircuit.

2.4. Matrix Method for Complex Hybrid Network Including Nonlinear and High Order Linear Elements

Complex hybrid networks comprised of linear and nonlinear elements have been used extensively in various microwave circuits and antenna systems. For instance, the diode and FET devices have been used frequently as mixers or oscillators and can be equivalent to a complex hybrid network. In order to model such a network, a FDTD model has been presented in [14, 15]. However, in complex hybrid network, when some elements are the high order ones (expressed by high order equations), these methods are ineffective. Combining Kirchhoff's circuit laws with Equations (4), (5), (9), and (10), the improved matrix method is able to extend to solve this problem. Because of existence of the nonlinear elements, a nonlinear equations set is used to describe the complex hybrid network. Its solution can be obtained by Newton-Raphson numerical method [15, 16]. The procedure to build and discretize the nonlinear equations set is basically the same as that in Subsection 2.3.

In the following context, two active antenna examples are analyzed to demonstrate the efficiency and applicability of the proposed approaches.

3. THE APPLICATION OF THE IMPROVED MATRIX METHOD TO ANTENNA ANALYSIS

3.1. The Wide-band Wire Antenna Loaded with Wide-band Match Network

The structure of the wire antenna is shown in Fig. 2. Its half length is $l = 5.0\,\mathrm{m}$, and the diameter of the metal wire is $D = 0.02\,\mathrm{m}$. The antenna is fed at its middle point. In order to obtain a good match characteristic, an impedance match network is added at the input port, and its detailed configuration is shown in Fig. 3(a). Three sets of different element parameters listed in Table 1 are used for matching the antenna at different operation frequency bands. In order to simplify the loaded network, a voltage source V_s'' and an impedance $R_0 = n^2 \cdot R_s\Omega$ are used in Fig. 3(b) instead of the original voltage source V_s', impedance R_s, and transformer. This network in Fig. 3(b) is the one with an internal independent voltage source. The antenna has been analyzed by MOM in [8]. The spatial increments $\Delta x = \Delta y = \Delta z = 0.04\,\mathrm{m}$ and time increment $\Delta t = 77\,\mathrm{ps}$ are selected for the improved FDTD method, respectively. We assume the network occupies one FDTD cell. Gedney's PML is used to truncate all of the radiation boundaries [17].

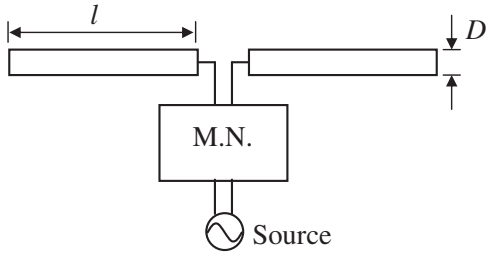

Figure 2. Structure of the wire antenna loaded with match network.

Table 1. Three sets match network parameters.

	L_1 (μH)	L_2 (μH)	L_3 (μH)	C_1 (PF)	C_2 (PF)	n
M. N. 1	0.027	0.017	93.05	2.72	17.75	1.863
M. N. 2	0.069	0.017	99.13	4.18	7.38	3.526
M. N. 3	0.048	0.21	95.6	0.30	0.012	4.811

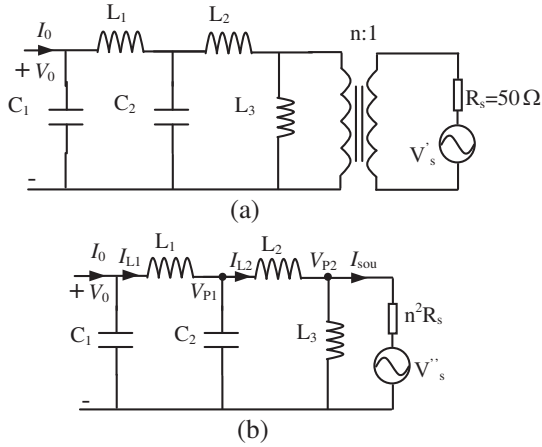

Figure 3. Loaded match network structure, (a) original structure and (b) simplified structure.

The relationship between the port voltage V_0 and port current I_0 can be deduced and expressed as

$$\begin{aligned}
&\frac{L_2L_1}{C_2R_0}\int I_0dt+\left(1+\frac{L_2}{L3}\right)\frac{L_1}{C_2}\iint I_0dt^2\\
&+\frac{L_1+L_2}{R_0}\iiint I_0dt^3+\left(1+\frac{L_1+L_2}{L_3}\right)\iiiint I_0dt^4\\
&=\frac{1}{R_0}\iiiint V_s''dt^4+C_1\frac{L_1L_2}{C_2R_0}V_0+C_1\left(1+\frac{L_2}{L3}\right)\frac{L_1}{C_2}\int V_0dt\\
&+\left(\frac{L_1+L_2}{R_0}C_1+\frac{L_2}{R_0C_2}\right)\iint V_0dt^2\\
&+\left[C_1\left(1+\frac{L_1+L_2}{L_3}\right)+\left(1+\frac{L_2}{L3}\right)\frac{1}{C_2}\right]\iiint V_0dt^3\\
&+\frac{1}{R_0}\iiiint V_0dt^4+\frac{1}{L_3}\iiiiint V_0dt^5
\end{aligned}\tag{18}$$

In this equation, the coefficients of $\int\ldots V_0dt^m$ and $\int\ldots I_0dt^r$ correspond to b_m and a_r according to Equations (2) and (3). From Norton equivalent principle and Equation (18), it can be found that the relationship between Norton equivalent current source I_{so}^1 and independent V_s'' in the network can be expressed as follow

$$\begin{bmatrix}\frac{L_2L_1}{C_2R_0}\int I_{so}^1dt+\left(1+\frac{L_2}{L3}\right)\frac{L_1}{C_2}\iint I_{so}^1dt^2\\+\frac{L_1+L_2}{R_0}\iiint I_{so}^1dt^3+\left(1+\frac{L_1+L_2}{L_3}\right)\iiiint I_{so}^1dt^4\end{bmatrix}=-\frac{1}{R_0}\iiiint V_s''dt^4 \tag{19}$$

Because of single internal source in this network, the second item of the right side in Equation (15) can be written as

$$S_I = \sum\nolimits_{r=0}^{R} a_r I_{so}^1(s)\,(1/s)^r \tag{20}$$

The expression at the left side of Equation (19) is just the inverse Fourier transform of (20). Therefore, the inverse Fourier transform of the second item of the right side in Equation (15) can be substituted with the item at the right side in Equation (19). Then the constant volume matrix $\mathbf{C}_0^s$ in Equation (17) can be computed simply, and the required electronic field at the location of the match network can be calculated by the method presented in Subsection 2.2. This analysis has also demonstrated the physical meaning of the first item at the right side in Equation (18). In order to calculate the match characteristic of the antenna, the time domain information at the source port should be obtained. From Fig. 3(b), the following discretized equations can be used to calculate the voltage V_{p2} and current I_{sou} of the source port

$$I_{L1}^{n+1/2} = I_0^{n+1/2} - C_1\left(V_0^{n+1} - V_0^n\right)/\Delta t \tag{21a}$$

$$V_{P1}^n = V_0^n - L_1\left(I_{L1}^{n+1/2} - I_{L1}^{n-1/2}\right)/\Delta t \tag{21b}$$

$$I_{L2}^{n+1/2} = I_{L1}^{n+1/2} - C_2\left(V_{P1}^{n+1} - V_{P1}^n\right)/\Delta t \tag{21c}$$

$$V_{P2}^n = V_{P1}^n - L_2(I_{L2}^{n+1/2} - I_{L2}^{n-1/2})/\Delta t \tag{21d}$$

$$I_{sou}^n = I_{L2}^n - (1/L_3)\sum\nolimits_{i=0}^{n} V_{P2}^i \Delta t \tag{21e}$$

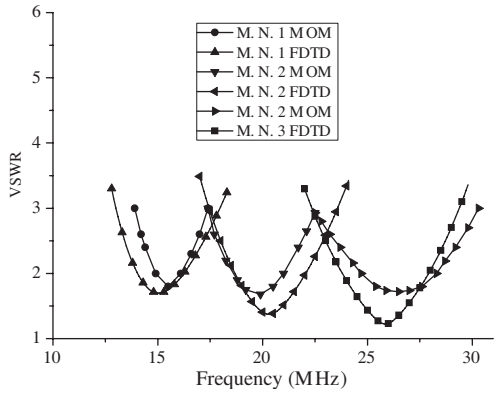

Figure 4. VSWR of the loaded antenna with different match network.

The VSWR extracted from V_{p2} and I_{sou} is shown in Fig. 4. The results from MOM [8] are also demonstrated as a reference. It is seen that they are in good agreement with each other. So, the developed FDTD model for linear lumped network including internal independent sources is effective and accurate.

Certainly, the loaded lumped network in this antenna can also be analyzed by the method introduced in Subsection 2.3 in order to avoid the mathematic operations for network equation and internal independent source. If just the nodal voltages or branch currents in the network are regarded as the unknowns, some equations from Kirchhoff's laws are the high order ones, and the transform (4) and (5) must be used to discretize them. The analyses have indicated that the two models in Subsections 2.2 and 2.3 can yield the same results.

The condition numbers of matrix $\mathbf{A}$ based on the improved FDTD method in Subsection 2.2 and matrix $\mathbf{A}'$ based on Equations (6) and (7) are compared to evaluate the algorithmic stability. The condition numbers of matrixes $\mathbf{A}$ and $\mathbf{A}'$ with different time increment Δt are listed in Table 2. From this table, it can be deduced that the stability of the proposed FDTD method is improved markedly compared with the traditional method. Meanwhile, the stability of the proposed FDTD method is improved further as Δt reduces. However, it is uncertain for the traditional method because its condition number of matrix $\mathbf{A}'$ becomes worse as Δt is reduced in some cases, e.g., M.N.1.

Table 2. Comparison of the condition number of matrix $\mathbf{A}$ and $\mathbf{A}'$.

Matrix		Condition number		
		$\Delta t = 77\,\text{ps}$	$\Delta t = 7.7\,\text{ps}$	$\Delta t = 0.77\,\text{ps}$
M. N. 1	A_1	$4.3e+23$	$6.8e+22$	$3.2e+21$
	A_1'	$1.8e+41$	$2.2e+41$	$3.8e+41$
M. N. 2	A_2	$5.5e+22$	$1.1e+22$	$3.1e+21$
	A_2'	$1.2e+41$	$3.7e+40$	$3.7e+38$
M. N. 3	A_3	$1.0e+021$	$1.5e+20$	$1.5e+19$
	A_3'	$1.3e+41$	$2.5e+38$	$1.4e+36$

3.2. Two-element Active Antenna Loaded with Gunn Diodes

Using the improved matrix type FDTD method, an example of the two-element active patch antenna shown in Fig. 5 is analyzed. The two elements of the antenna are connected by a coupling line. One Gunn

diode is integrated in each element to generate microwave signals. The antenna patches are supported by microstrip substrate with a relative permittivity ε_r and a thickness h. This antenna has been researched in [18] and analyzed by the traditional FDTD method in [19–23]. The configuration parameters are listed in Table 3. The spatial increments are selected as $\Delta x = 0.24\,\text{mm}$, $\Delta y = 0.31\,\text{mm}$ and $\Delta z = 0.263\,\text{mm}$, respectively, and the time increment $\Delta t = 0.5\,\text{ps}$ is selected in FDTD simulation.

The equivalent circuit of the quasi ideal-packaged Gunn diodes D_1 and D_2 in Fig. 5 is the part enclosed in dotted box in Fig. 6. In Fig. 6, I_s is a nonlinear current source and can be expressed by

$$I_s = -G_1 V_c + G_3 V_c^3 \tag{22}$$

Firstly, the active antenna loaded with the quasi ideal-packaged Gunn diodes is analyzed. In terms of Kirchhoff's laws, the circuit

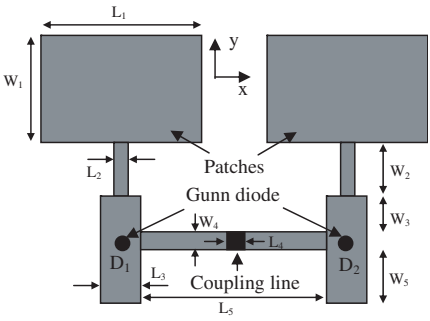

Figure 5. Layout of the two-element patch antenna.

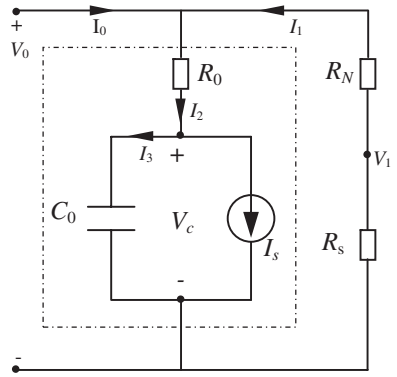

Figure 6. Equivalent circuit model of the loaded Gunn diode.

Table 3. Configuration parameters of the two-element microstrip antenna.

$L_1 = 10.8\,\text{mm}$	$L_2 = 0.24\,\text{mm}$	$L_3 = 2.16\,\text{mm}$	$L_4 = 0.48\,\text{mm}$
$L_5 = 17.76\,\text{mm}$	$W_1 = 8.37\,\text{mm}$	$W_2 = 5.27\,\text{mm}$	$W_3 = 3.72\,\text{mm}$
$W_4 = 2.48\,\text{mm}$	$W_5 = 5.58\,\text{mm}$	$h = 0.79\,\text{mm}$	$\varepsilon_r = 2.33$

equations of the device are

$$I_2 - I_3 - I_s = 0 \tag{23a}$$

$$V_0 - V_c - I_2 R_0 = 0 \tag{23b}$$

$$C_0 V_c - \int I_3 dt = 0 \tag{23c}$$

I_2 and V_0 are the port current and port voltage of the quasi ideal-packaged diode, respectively. Assuming each loaded diode occupies one FDTD cell, Equations (23a) and (23b) can be discretized as

$$I_2^{n+1/2} - I_3^{n+1/2} - I_s^{n+1/2} = 0 \tag{24}$$

$$\left(V_0^{n+1} - V_c^{n+1}\right)/2 - I_2^{n+1/2} R_0 + (V_0^n - V_c^n)/2 = 0 \tag{25}$$

Based on the transform (4) and (5), Equation (23c) should be discretized as the following equations,

$$C_0 V_s^{n+1} - \Delta t I_{31}^{n+1/2} = 0 \tag{26a}$$

$$I_{31}^{n+1/2} - \frac{1}{2} I_3^{n+1/2} - \left(I_{31}^{n-1/2} + \frac{1}{2} I_3^{n-1/2}\right) = 0 \tag{26b}$$

Then, combining Equations (22) and (24)–(26) with Equations (9) and (10), a nonlinear equations set can be constructed. By Newton-Raphson method, the required fields can be solved conveniently.

The circuit parameters in Equations (22) and (23) are: $G_1 = 0.0252\,\Omega^{-1}$, $G_3 = 0.0265\,\Omega^{-1}\mathrm{V}^{-1}$, $R_0 = 1.0\,\Omega$ and $C_0 = 0.2\,\mathrm{pF}$, respectively. In this example, only the case that the coupling line in Fig. 5 is an ideal metal pad is considered. As excitement, a small amount of numerical noise is introduced into the FDTD cell. The simulated total voltage across the diode D_1 is shown in Fig. 7. From the simulated voltage signal, it can be found that the resonant voltage amplitude of the Gunn diodes and the resonant frequency of the antenna system are 1.125 V and 12.38 GHz, respectively, which are the same as those of [19]. This procedure also indicates that the improved method is effective and accurate.

Now another parasitic effect on the Gunn diodes is considered and is equivalent to an additional shunt circuit, as shown in Fig. 6. This parasitism can be caused by a non-ideal packaging of the Gunn diodes. In this shunt circuit, $R_s = 100\,\Omega$, R_N is a high order network and expressed with

$$R_N = \frac{A_1(1/s)}{B_0 + B_2 \times (1/s)^2}, \tag{27}$$

where A_1=1, $B_0 = 8.85 \times 10^{-13}$ and $B_2 = 5 \times 10^9$, respectively. Obviously, it is very difficult, if not impossible, for the traditional

FDTD method to model this complicated hybrid network [12, 15]. However, it is straightforward to model this device by the improved matrix type FDTD technique. Besides Equations (9), (10), and (24)–(26), the additional equations required to describe the complex hybrid network are

$$V_1 - V_0 - R_N I_1 = 0 \tag{28a}$$

$$I_0 + I_1 - I_2 = 0 \tag{28b}$$

$$V_1 + I_1 R_s = 0 \tag{28c}$$

Equation (28a) should be discretized as the following equations by transform (3)–(5)

$$B_0 V_1^{n+1} + B_2(\Delta t)^2 V_{12}^{n+1} - \left(B_0 V_0^{n+1} + B_2(\Delta t)^2 V_{02}^{n+1}\right) - A_1 \Delta t I_{11}^{n+1/2} = 0 \tag{29a}$$

$$V_{11}^{n+1} - \frac{1}{2} V_1^{n+1} - \left(V_{11}^n + \frac{1}{2} V_1^n\right) = 0 \tag{29b}$$

$$V_{12}^{n+1} - \frac{1}{2} V_{11}^{n+1} - \left(V_{12}^n + \frac{1}{2} V_{11}^n\right) = 0 \tag{29c}$$

$$V_{01}^{n+1} - \frac{1}{2} V_0^{n+1} - \left(V_{01}^n + \frac{1}{2} V_0^n\right) = 0 \tag{29d}$$

$$V_{02}^{n+1} - \frac{1}{2} V_{01}^{n+1} - \left(V_{02}^n + \frac{1}{2} V_{01}^n\right) = 0 \tag{29e}$$

$$I_{11}^{n+1/2} - \frac{1}{2} I_1^{n+1/2} - \left(I_{11}^{n-1/2} + \frac{1}{2} I_1^{n-1/2}\right) = 0 \tag{29f}$$

(28b) and (28c) can be discretized by the ordinary method.

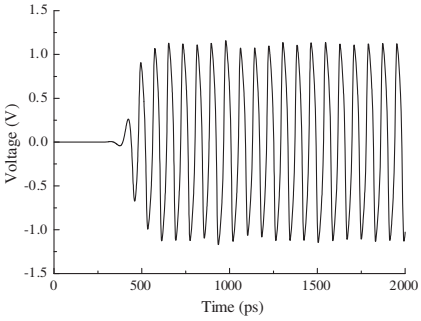

Figure 7. Time development of the total voltage across the diode D_1 when the quasi-ideal packaged diode model is used.

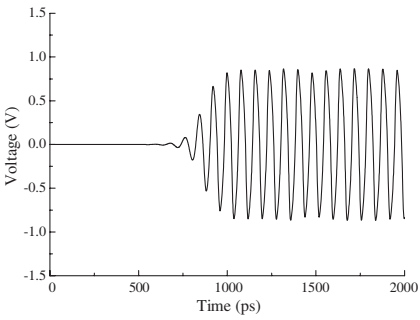

Figure 8. Time development of the total voltage across the diode D_1 when another parasitic shunt circuit is added.

Newton-Raphson method is used to resolve nonlinear equations set. Fig. 8 shows the simulated voltage across the first diode D_1. Due to the effect of parasitic shunt circuit, the resonant voltage amplitude of the Gunn diode has changed from 1.125 V to 0.856 V, and the resonant frequency of the antenna system has also shifted from 12.38 GHz to 12.52 GHz. The voltages across the diode D_1 and D_2 indicate that the two patch antenna elements operate with out-of-phase mode [19].

The performance of the Jacobian matrix $\mathbf{A_J}$ in Newton-Raphson method has also been analyzed in the example in which the parasitism effect is considered. The Jacobian matrix $\mathbf{A_J}$ is changeable slightly at different time updates, and its typical condition number has been listed in Table 4. For the purpose of comparison, the typical condition number of the Jacobian matrix $\mathbf{A'_J}$ based on the traditional transform (6) and (7) has been listed in Table 4. Table 4 has also given the typical and maximum iteration times at the time updates when Newton-Raphson numerical method is used to solve the nonlinear equations set. From Table 4, it is clear that the matrixes based on transform (4) and (5) are more well-conditioned than those based on transform (6) and (7), and the improved matrix type FDTD method needs less computational time.

In this paper, our experience has demonstrated that when the time and spatial increments satisfy traditional Courant condition, the improved matrix type FDTD method is stable.

Table 4. Comparison between the novel matrix and the traditional one.

Matrix	Typical Condition umber	iterate times with $\sum B(i)^2 < 1.0e^{-10}$	
		Typical	Maximum
$\mathbf{A_J}$	$1.0e+22$	9	10
$\mathbf{A'_J}$	$1.0e+26$	12	138

4. CONCLUSION

The application of the improved matrix type FDTD method has been extended further to analyze the antenna loaded with complex lumped and hybrid network in this paper. A simple FDTD model for linear lumped networks including internal independent sources is developed, and as an example, a wire antenna loaded with a wide band-matched

lumped network is analyzed using this model. The complex hybrid networks which compose of nonlinear and high order linear elements with arbitrary connection can be also analyzed by the developed method, and a diode-loaded two-element patch antenna is selected to demonstrate the application. Due to the new integral transform technique, the coefficient matrixes $\mathbf{A}$ of the complex linear lumped networks and the Jacobian matrixes $\mathbf{A}'_{\mathbf{J}}$ of the complicated hybrid networks are much more well-conditioned than those of the traditional method, respectively. The example of the diode-loaded patch antenna has also indicated that the improved matrix type FDTD method is more time-saving than the traditional one for the analysis of complex hybrid network.

ACKNOWLEDGMENT

This work was supported in part by the New-century Talent Program of the Education Department of China under grant NCET070154, in part by the National Defense Research Funding under grant 08DZ0229 and 09DZ0204, in part by the Hi-Tech Research and Development Program of China under grant 2009AA01Z231 and in part by the Funding of National Key Laboratory of Millimeter Wave under grant K200809.

REFERENCES

1. Taflove, A. and S. C. Hagness, *Computational Electrodynamics: The Finite-difference Time-domain Method*, 3rd edition, Artech House, Norwood, MA, 2005.
2. Jin, J., *The Finite Element Method in Electromagnetics*, 2nd edition, CRC Press, Boca Raton, FL, 2002.
3. Mittra, R. and K. Du, "Characteristic basis function method for iteration-free solution of large method of moments problems," *Progress In Electromagnetics Research B*, Vol. 6, 307–336, 2008.
4. Xiao, S. Q., Z. H. Shao, M. Fujise, and B.-Z. Wang, "Pattern reconfigurable leaky-wave antenna design by FDTD method and Floquet's theorem," *IEEE Trans. Antennas Propag.*, Vol. 53, 1845–1848, May 2005.
5. Wang, M. Y., J. Xu, J. Wu, B. Wei, H.-L. Li, T. Xu, and D.-B. Ge, "FDTD study on wave propagation in layered structures with biaxial anisotropic metamaterials," *Progress In Electromagnetics Research*, PIER 81, 253–265, 2008.
6. Sabri, M. M., J. Rashed-Mohassel, and N. Masoumi, "Application of FDTD-based macromodeling for signal integrity analysis in

practical PCBs," *Progress In Electromagnetics Research Letters*, Vol. 5, 45–55, 2008.

7. Khajehpour, A. and S. A. Mirtaheri, "Analysis of pyramid EM wave absorber by FDTD method and comparing with capacitance and homogenization methods," *Progress In Electromagnetics Research Letters*, Vol. 3, 123–131, 2008.
8. Yegin, K. and A. Q. Martin, "On the design of broad-band loaded wire antennas using the simplified real frequency technique and a genetic algorithm," *IEEE Trans. Antennas Propag.*, Vol. 51, 220–228, Feb. 2003.
9. Sui, W., D. A. Christensen, and C. H. Durney, "Extending the two-dimensional FDTD method to hybrid electromagnetic system with active and passive lumped elements," *IEEE Trans. Microwave Theory Tech.*, Vol. 40, 724–730, Apr. 1992.
10. Pereda, J. A., F. Alimenti, P. Mezzanotte, L. Roselli, and R. Sorrentino, "A new algorithm for the incorporation of arbitrary linear lumped networks into FDTD simulators," *IEEE Trans. Microwave Theory Tech.*, Vol. 47, 943–949, Jun. 1999.
11. Wu, T.-L., S.-T. Chen, and Y.-S. Huang, "A novel approach for the incorporation of arbitrary linear lumped network into FDTD method," *IEEE Microwave and Wireless Components Letters*, Vol. 14, 74–76, 2004.
12. Kuo, C.-N., B. Houshmand, and T. Itoh, "Full-wave analysis of package microwave circuits with active and nonlinear devices: An FDTD approach," *IEEE Trans. Microwave Theory Tech.*, Vol. 45, 819–826, May 1997.
13. Shao, Z. H. and M. Fujise, "An improved FDTD formulation for general linear lumped microwave circuits based on matrix theory," *IEEE Microw. Theory Tech.*, Vol. 53, 2261–2266, July 2005.
14. Su, D. Y., D.-M. Fu, and Z.-H. Chen, "Numerical modeling of active devices characterized by measured S-parameters in FDTD," *Progress In Electromagnetics Research*, PIER 80, 381–392, 2008.
15. Koh, B. P., I. J. Graddock, P. Urwin-Wright, and C. J. Railton, "FDTD analysis of varactor-tuned patch antenna including device packaging effects," *IEE Electronics Letters*, Vol. 37, 1494–1495, Dec. 2001.
16. Sui, W., *Time-domain Computer Analysis of the Nonlinear Hybrid Systems*, CRC Press, New York, 2002.
17. Li, J., L. Guo, and H. Zeng, "FDTD investigation on bistatic scattering from a target above two-layered rough surfaces using UPML absorbing condition," *Progress In Electromagnetics*

Research, PIER 88, 197–211, 2008.

18. Nogi, S., J. Lin, and T. Itoh, "Mode analysis and stabilization of a spatial power combining array with strongly coupled oscillators," *IEEE Trans. Microwave Theory Tech.*, Vol. 41, 819–826, Oct. 1993.
19. Thomas, V. A., K.-M. Ling, M. E. Jones, B. Toland, J. Lin, and T. Itoh, "FDTD analysis of an active antenna," *IEEE Microwave and Guided Wave Letters*, Vol. 4, 296–298, Sep. 1993.
20. Emili, G., F. Alimenti, P. Mezzanotte, L. Roselli, and R. Sorrentino, "Rigorous modeling of packaged Schottky diodes by the nonlinear lumped network (NL2N)-FDTD approach," *IEEE Trans. Microwave Theory Tech.*, Vol. 48, 2277–2282, Jan. 2000.
21. Ei Mrabet, O. and M. Essaaidi, "An efficient algorithm for the global modeling of RF and microwave circuits using a reduced nonlinear lumped network (RNL2N)-FDTD approach," *IEEE Microwave and Wireless Components Letters*, Vol. 14, 86–88, Feb. 2004.
22. Vahabi Sani, N., A. Mohammadi, A. Abdipour, and F. M. Ghannouchi, "Analysis of multiport receivers using FDTD technique," *Journal of Electromagnetic Waves and Applications*, Vol. 23, No. 5–6, 635–643, 2008.
23. Liu, H. and H. W. Yang, "FDTD analysis of magnetized ferrite sphere," *Journal of Electromagnetic Waves and Applications*, Vol. 22, No. 17–18, 2399–2406, 2008.